EARTH OBSERVATION AND GEOMATICS ENGINEERING

website: https://eoge.ut.ac.ir

Investigating land subsidence in the Sarkhun gas field using Persistent Scatterer Interferometry

Zahra Azargoshayesh [1]* Amirshahrokh Amini [2]

[1] Department of Remote Sensing, Faculty of Technical Engineering, South Tehran Branch, Islamic Azad University, Tehran, Iran

[2] Department of Remote Sensing, Faculty of Technical Engineering, South Tehran Branch, Islamic Azad University, Tehran, Iran

Article history:
Received: 29 December2022, Received in revised form: 12 May 2023, Accepted: 15 May 2023

ABSTRACT

Land subsidence due to gas extraction in the Sarkhun gas field, 20 km northeast of Bandar Abbas, Iran, is investigated and evaluated in this study. For this purpose, the Stanford Method for Persistent Scatterers (StaMPS) package was employed to process 46 descending Sentinel-1A satellite images were collected between 20190111 to 20220309, and 28 ascending Sentinel-1A satellite images collected between 20200111 to 20220217 to extract the displacement along the line of sight of the satellite and due to the occurrence of an earthquake on November 14, 2021 near the gas field with a magnitude of 6.4 and 6.3 in Fin city of Hormozgan province, land surface deformation was measured in the two stages before and after the earthquake for each track to understanding the effect of the earthquake on the behavior of displacement in the study area, and the presence of subsidence in the Sarkhun gas field was seen in the results of the two tracks. The calculated subsidence results for two tracks, descending 166 and ascending 57, and for before and after the earthquake are: During the years 20190111 to 20211028 along the LOS for descending data until before the earthquake is between 6.8 and -9.1 mm per year and during the years 20190111 to 20220309, until after the earthquake is between 5.8 and -7.2 mm per year. During the years 20200111 to 20211113 along the LOS for ascending data before the earthquake is between -23.4 and 12.9 mm per year and during the years 20200111 to 20220217, after the earthquake is -17.4 and 11.1.

KEYWORDS

Sarkhun gas field
time series analysis
persistent scatterers
land subsidence
StaMPS

1. Introduction

Subsidence is actually the downward movement of the earth's surface as a result of natural factors or factors caused by human activities, natural factors such as volcanic activity, earthquakes, land collapse in the place of soluble land, and human factors caused by mining, underground water extraction, oil and gas extraction and construction (Sharifikiya, 1391). This phenomenon has harmful effects on many structures and infrastructures in urban areas and their suburbs, such as bridges, buildings, refineries, water supply lines, gas and sewage lines, and power transmission lines (Mirzaii et al., 2019). In addition to the environmental consequences, the displacement of the earth's crust causes changes in the topography and hydraulic characteristics of the region, an increase in the degree of flooding with a decrease in the degree of soil permeability, and a change in the state of the earth such as the direction and speed of underground water flows (Mirzaii et al., 2019). Due to the dry climatic conditions of our country, which has few water reserves and on the other hand, it has rich oil and gas resources, as a result, due to excessive harvesting of these

reserves, subsidence is prone to occur both in the plains and in the areas that are used for oil and gas extraction.

And subsidence has become a destructive and problematic phenomenon for the country in the past years. In this regard, it is necessary to monitor the areas under the risk of subsidence to identify its behavior in time and its spatial extent continuously and with modern and accurate methods of the day with available data. The first major cause of subsidence in Iran is the uncontrolled withdrawal of underground water, which has caused subsidence in many plains of the country, such as the subsidence of Neishabour Plain, Rafsanjan, Mashhad, Kerman, Kabudar Ahang Plain, southwest of Tehran, which in recent years, during various researches, researchers have measured the amount of subsidence in these plains (Dehghani et al., 2009, 2013; Motagh et al., 2007, 2008, 2017; Mousavi et al., 2001). One aspect is the investigation of the vast subsidence of the Tehran plain caused by the indiscriminate extraction of underground water sources, which causes the subsidence of the southwestern region of Tehran with a maximum subsidence rate of 36 cm per year, which is one of the highest subsidence rates in the world. And secondly, the investigation of local subsidence to a smaller extent but in densely populated urban areas due to other factors such as underground constructions and wear and tear of old infrastructures has been investigated (Samiei Esfahany & Ajourlou, 2018).

In the last decade, researchers investigated and measured the subsidence caused by oil extraction in some oil fields such as the Azar oil field, Maron oil field, Durood oil field, Naft Shahr oil field, and Aghajari oil field (Mirzaii et al., 2019; Fathollhi et al., 1397; FouladiMogadam et al., 2011; Mohammadi et al., 1389).

In other parts of the world, researchers are carefully focusing on monitoring the subsidence in oil and gas fields and studying these fields with accurate modern methods such as radar interferometry. As an example, we can mention the Lost Hills oil field, which has a long history in oil and gas extraction, has and suffers from long-term deformation (Shi et al., 2022). In the Gudong oil field located in the Yellow River Delta, the second largest river delta in China, researchers used the Stanford Method for persistent scatterers (StaMPS) to investigate the subsidence phenomenon. Subsidence in river deltas is a complex process that has both natural and human causes. The increase in human activities such as aquaculture and oil extraction in the Yellow River Delta, has caused subsidence in this area. Field investigation shows the connection between non-uniform subsidence areas and oil extraction (Liu et al., 2015). The images of three satellites Sentinel-1, Cosmo-SkyMED, and TerraSAR-X were used to detect vertical subsidence in the Tengiz oil field of Kazakhstan (Bayramov et al., 2022).

In this study, the subsidence caused by gas extraction in the Sarkhun gas field and the effect of the earthquake of November 14, 2021 on the behavior of subsidence in the studied area has been investigated. The purpose of this study is to investigate the presence and occurrence of subsidence due to gas extraction and the influence of earthquakes on the behavior of subsidence. For this purpose, persistent scattering interferometry, using the Stanford Method for Persistent Scatterers (StaMPS) with the help of Sentinel 1-A satellite images, has been selected for estimating subsidence. Due to the short period of time to receive radar images, suitable spatial accuracy, and especially the shorter spatial baseline and availability, Sentinel-1A radar images for the period of 2019 to early 2022 were selected for this study.

2. Area of study

The Sarkhun gas field is located in Hormozgan province, 20 kilometers northeast of Bandar Abbas, where the presence of gas was proved by drilling the first well in 1351. On average, this field is 27.75 km long and 7.5 km wide, between 56.35 and 56.45 longitudes and 27.29 and 27.37 latitudes. Sarkhun field has two reservoirs named Gouri-Bazdeh and Jahrom-Razak, and production from Sarkhun field has started since the end of 1365, and the gas produced by the wells is for processing to Sarkhun and Qeshm gas refineries next to the field and after that, for urban, industrial consumption and gas power plants in the provinces of the southeast of the country is sent.

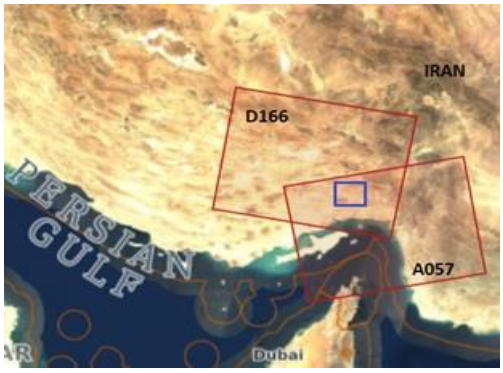

Figure 1. The blue box is the Sarkhun gas field; the red boxes are descending orbit images D166 and ascending orbit images A057.

3. Data and methods of use

Interferometric Synthetic Aperture Radar (InSAR) time series techniques are powerful geodetic remote sensing approaches for estimating millimetric surface deformation from space (Hanssen, 2001a). InSAR is a well-known geodetic technique that has been widely used to measure and monitor land deformation in different regions for several decades (Hooper et al., 2012). The wide spatial coverage, the ability to collect data during the day and night, and the possibility of measuring deformation in time intervals from days to decades using stored images have made InSAR an efficient technique compared to other geodetic methods.

InSAR uses phase difference observations between two radar acquisitions to estimate surface deformation. In addition to the desired deformation signal, the interferometric phase also includes residual topography and orbital errors, atmosphere, and noise (Hanssen, 2001b) . After all, only the fractional phase is observed, which

indicates that the number of integer cycles from the satellite to the ground surface is unknown.

Persistent scatterer interferometry (PSI) was first introduced by Ferrety in 2000, and 2001. Persistent scatterers are targets with a coherent phase behavior in time that often corresponds to human-made effects on the Earth. Phase difference observations from persistent scatterers are used for a specific estimate of the deformation signal and other phase contributions, such as topographic height differences and atmospheric disturbances. In addition, they form a network of reliable measurement points where phase unwrapping is performed. Persistent scatterer interferometry (PSI) has been successfully applied in urban areas where PS density is high. PSI has been used to estimate deformation caused by various causes: subsidence caused by water pumping, mining activities, hydrocarbon production, and landslides ((Gini) Ketelaar, 2009).

In this study, the StaMPS method has been used to investigate the existence and occurrence of subsidence phenomenon in the study area. This algorithm is based on the phase characteristics and allows the detection of stable pixels in areas where amplitude-based algorithms may fail. By using this approach, a larger density of PS is found in certain areas (e.g., vegetated, cropping lands) in comparison to the Ferretti et al. (2001) approach. Contrary to other PSI algorithms, this method uses only the spatially correlated nature of the deformation, and no a priori assumptions about its temporal behavior are done (Siles, 2015). Moreover, this method has been proven to work also with a few SAR acquisitions (Hooper et al., 2004).

The task of PSI algorithms is to identify the pixels that are dominated by a single dominant scatterer in order to extract the phase information contained in the interferometric phase. The StaMPS algorithm selects PS based on phase stability analysis, which makes it a powerful tool compared to amplitude based methods (Adam et al., n.d.; Hooper, 2008; Sousa et al., 2011). Because a higher PS density has been obtained in this method.

Pixels with low SNR can actually have a stable scatter. However, due to variations in the scattering properties of surrounding scatterers in the same resolution cell, the target pixel is characterized by a noisy phase. While the scatter-based algorithms do not consider the amplitude of this pixel, but StaMPS considers these pixels in the PS analysis, which primarily selects PSs including two steps:
a) amplitude phase discrimination, and b) phase stability selection.

Although StaMPS uses phase stability analysis to select the final PSs, it has minimized the initial selection of improbable PSs and thus reduced the data processing time (Siles, 2015). It has an amplitude-based measurement for early detection of PS. For this purpose, the dispersion index D_A is used. The D_A threshold in StaMPS is usually set higher than the value suggested by (Ferretti et al., 2001). After the initial selection of PSs, they are sent to the phase stability analysis step. An additional step is also included to analyze pixels with a higher D_A threshold limit than the initially determined threshold limit (Siles, 2015).

The interferometric phase is masked by many components: atmosphere, topography, orbit ramp, and noise. By using an external DEM and orbital information the topographic and orbital contributions can be extracted. Then, the differential phase in the interferogram can be expressed as follows,

$$\emptyset_{\text{int}} = \emptyset_{\text{def}} + \Delta\emptyset_{\epsilon} + \emptyset_{\text{atm}} + \Delta\emptyset_{\text{orb}} + \text{n}$$

where now $\Delta\emptyset_{\epsilon}$ and $\Delta\emptyset_{orb}$ are the height and geometrical residuals due to the use of an inaccurate topographic model and imprecise orbit information, respectively. $\emptyset_{atm}$ is the atmospheric effect between the two passes and n, is the noisy term due to different decorrelation sources (Hooper et al., 2004).

In this research, the data of Sentinel-1A was used in two tracks 166 descending and 57 ascending to investigate the occurrence of subsidence in the gas field. 166 track was used to check whether the subsidence phenomenon occurred due to gas extraction in the studied area or not, and 57 track was used to check the results of 166 track to see if there is a displacement signal on this track, and on the other hand, on November 14, 2021, earthquakes of magnitude 6.3 and 6.4 occurred in the city of Fin in Hormozgan province at the near gas field, with a short interval of time, so the calculation of the displacement in each track was carried out in two stages, the first stage before the earthquake and the second stage after the earthquake. 166 track includes 46 images taken from 20190111 to 20220309 in descending mode and 57 track includes 28 images taken from 20200111 to 20220217 in ascending mode.

Image 20200915 has been selected as the master image of descending 166 track and 20210129 as the master image of ascending 57 track (Figure 2).

All interferograms have been generated with respect to the master image in SNAP software (version 8) (SNAP Download – STEP, n.d.), and the correction of the topography phase contribution has been done by SRTM 1Sec HGT and the correction of the orbital error has been done by the accurate orbital information of the Sentinel satellite. And finally, from the interferograms produced in the SNAP software, the output is taken for processing the time series in the StaMPS software (version 4.1b) (StaMPS, n.d.), and from the StaMPS-Visualizer (Hoeser, 2018/2022) to see the time series of two points, one near the south side of the Sarkhun and Qeshm gas refinery on descending 166 track and the other on the southwest side of the gas refinery on ascending 57 track. The SNAP-StaMPS workflow chart is presented in Figure 3.

.

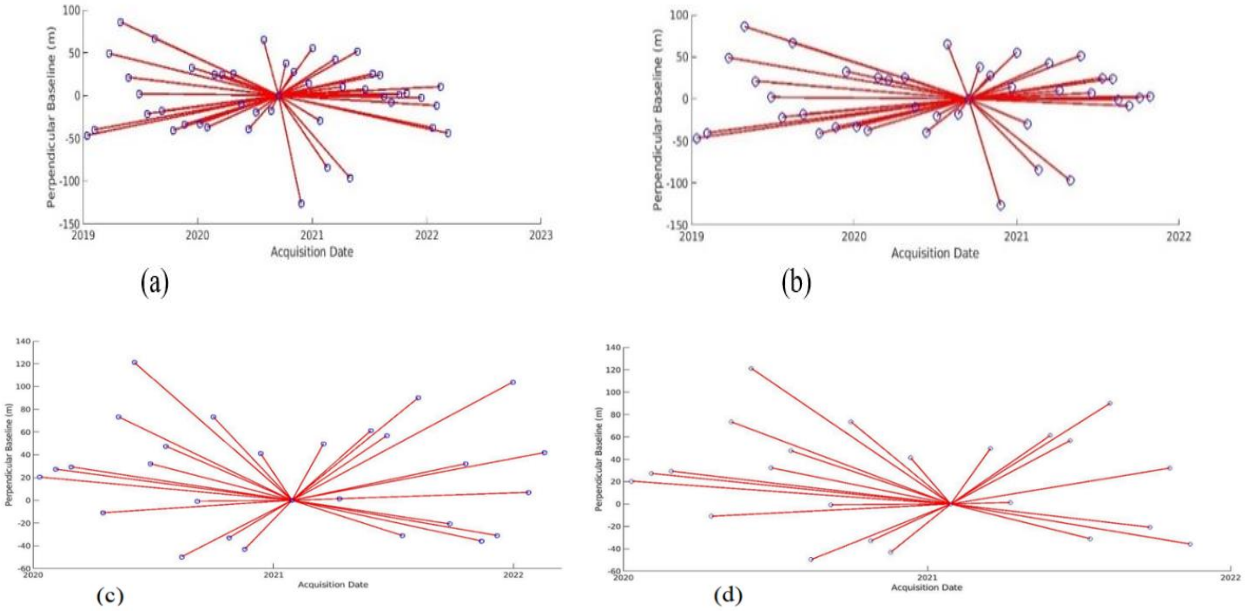

Figure 2. The single master network in Persistent Scatterer Interferometry (PSI), for the descending 166 track data set and the ascending 57 track data set, (a) with 46 images for after earthquake, 166 track, (b) with 41 images for before earthquake, 166 track (c) with 28 images for after earthquake, 57 track and (d) with 24 images for before earthquake, 57 track.

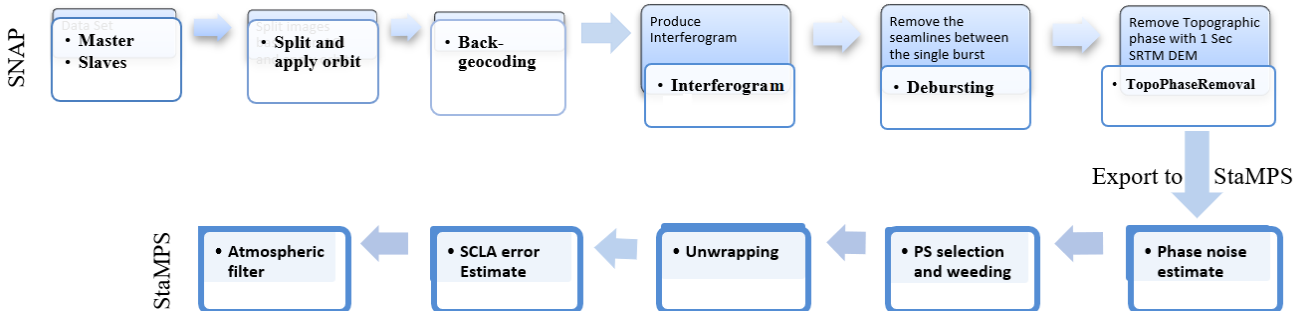

Figure 3. SNAP-StaMPS workflow chart

4. Results

Gas production from the Sarkhun gas field started in late 1365 and in 1384 with the drilling of the first well of the Razak reservoir, it was put into production, and its development program was implemented by drilling new wells and was put into operation, which increased production (Wikipedia). Gas field subsidence is usually large in area size and low in intensity, and the occurrence of an earthquake can cause an upward or downward jump in time while the subsidence rate remains constant.

4.1. descending 166 track data processing

4.1.1. Data processing with 41 images before the earthquake

The result of this processing for the descending 166 track data with 41 images before the mentioned earthquake is as Figure 4. The displacement rate during the years 20190111 to 20211028 along the LOS for the descending data before the earthquake is between -9.1 and 6.8 mm per year, as shown in Figure 4. The reference point with geographic coordinates lonlat= (56.32, 27.37) and with a radius of 250 meters which can be seen as a black star in the figure below. This point has been chosen as a reference point for both descending and ascending tracks.

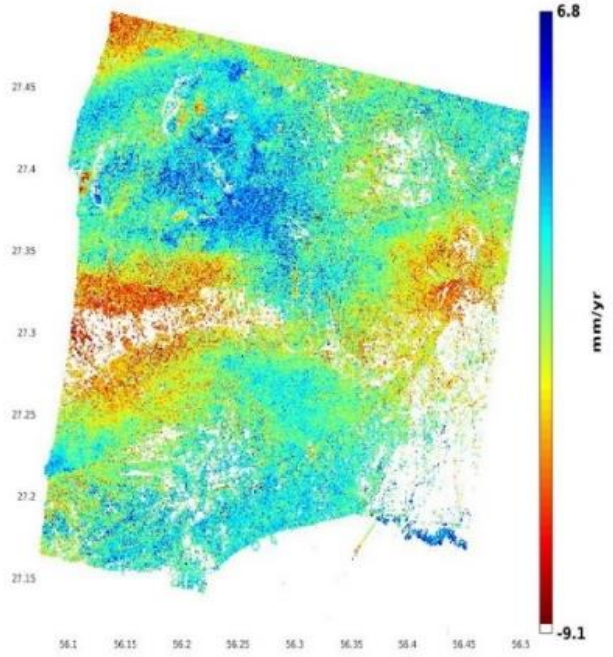

Figure 4. Deformation velocity map during the years 20190111 to 20211028 along the LOS for descending data until before the earthquake.

4.1.2. Data processing with 46 images after the earthquake of descending 166 track

The Figure below, the rate of displacement along the line of sight of the satellite is calculated after the earthquake. It is between -7.2 and 5.8 mm per year.

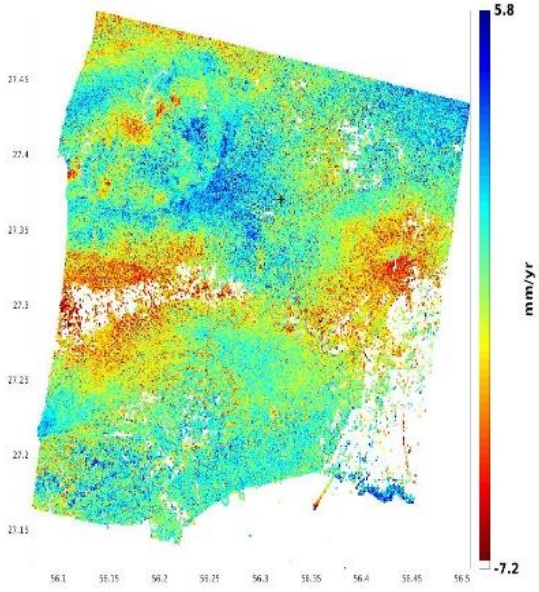

Figure 5. Deformation velocity map during the years 20190111 to 20220309 along the LOS for descending data until after the earthquake.

The Figure 6 shows the time series for a point near the

southern side of the Sarkhun and Qeshm refinery. The maximum subsidence value according to the time series of the selected point in Figure 6 can be seen on the date 20210902, it is about -29 mm.

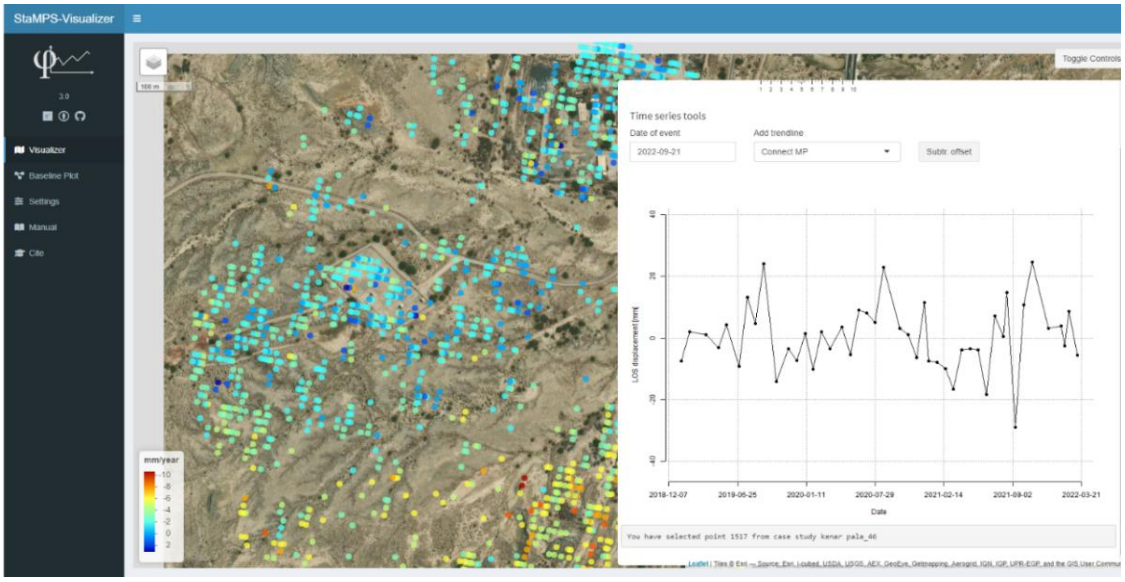

Figure 6. Time series of a location near the south side of the Sarkhun and Qeshm refinery on 166 track after the earthquake.

4.2. Results of ascending 57 track data processing

To validate whether the subsidence will be observed in the 57 track and the amount of this subsidence is consistent with the amount of subsidence of the 166 track or not. The StaMPS method was implemented for 28 images of the ascending 57 track and the following results were obtained, and the processing was performed before and after the earthquake and the results are presented as follows.

4.2.1. Data processing with 24 images of the ascending 57 tracks before the earthquake.

The results of this stage, which includes the displacement rate map between 20200111 and 20211113, are presented below. It is between -23.4 and 12.9 mm per year.

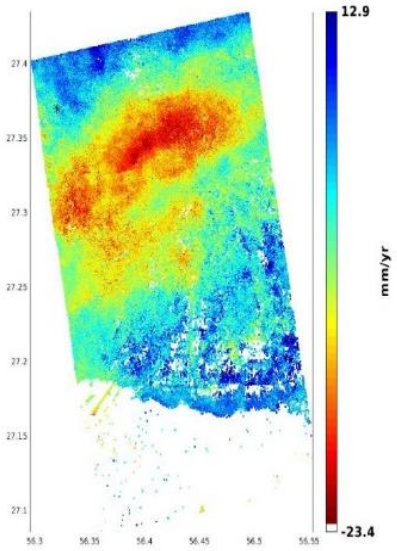

Figure 7. Deformation velocity map during the years 20200111 to 20211113 along the LOS for ascending 57 track before the earthquake.

4.2.2. Data processing with 28 images of the ascending 57 track after the earthquake.

The results of this stage, which includes the displacement rate map during the years 20200111 to 20220217, are presented below. It is between -17.4 and 11.1 mm per year.

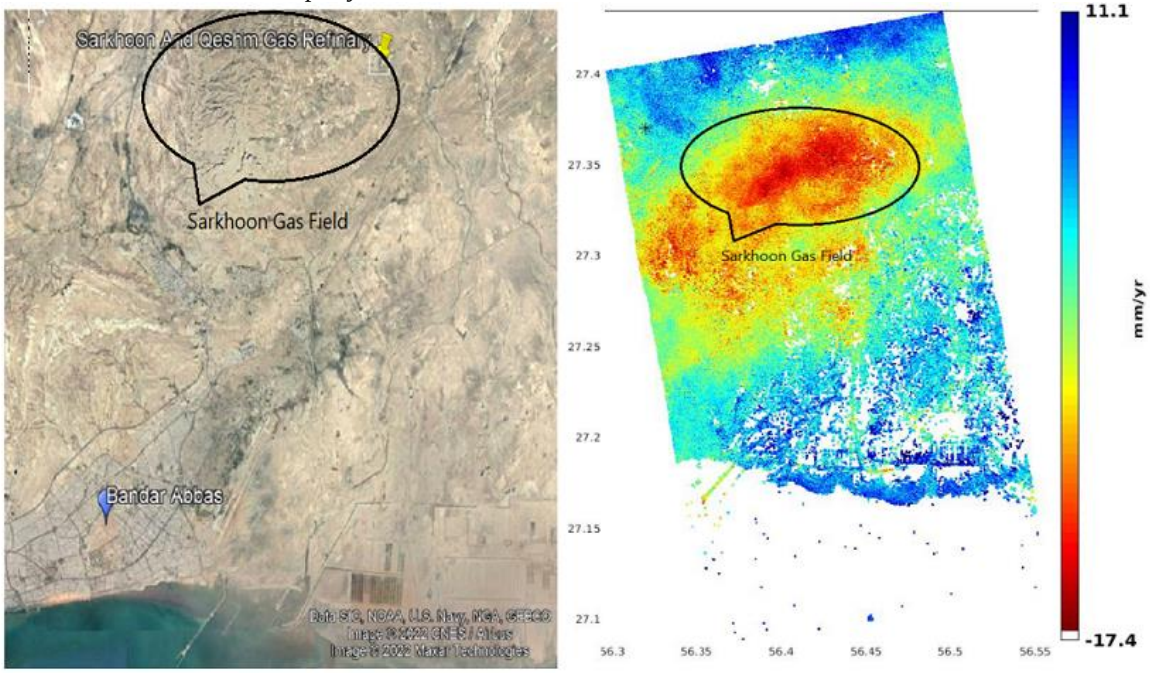

Figure 8. Deformation velocity map during the years 20200111 to 20220217 along the LOS for ascending 57 track data after the earthquake.

Figure 9 shows the time series for a point on the southwest side of Sarkhun and Qeshm refinery. The maximum subsidence value according to the time series of the selected point in Figure 9 can be seen around the date 20210902, it is about -39 mm.

.

Figure 9. Time series of a location in the southwest side of Sarkhun and Qeshm refinery on ascending 57 track after the earthquake.

5. Conclusions

This paper presents the application of InSAR time series processing to investigate land subsidence in the Sarkhun gas field. The method of persistent scatterers (StaMPS) was used to reveal the phenomenon of subsidence in the Sarkhun gas field due to gas extraction for many years and in two tracks, descending 166 and ascending 57, the subsidence phenomenon was seen and measured in the line of sight of the satellite. According to the earthquake that happened near the study area, the subsidence was calculated for each path before and after the earthquake, and the behavior of the surface deformation of the earth was seen almost the same in both paths.

By comparing the time series of two points near the Sarkhun and Qeshm gas refineries, one was chosen near the southern side of the refinery on 166 track and the other was chosen on 57 track in the southwest side of the refinery, the same results indicating the highest subsidence near the time of 20210902 for both track, that according to the opinion of an expert and specialist in the field of gas extraction from the gas company in Hormozgan province, that during the three years under study, there has been no increase in gas extraction from the field, however, we have seen a slight increase in the rate of subsidence in the field, which indicates that gas extraction has been a key factor.

Acknowledgements

The authors of this article are grateful to the European Space Agency for downloading Sentinel-1A images and Mr. Momeni, an expert in oil and gas extraction from Hormozgan province, for providing information on the amount of gas extraction during the three years under study.

References

Adam, N., Kampes, B., & Eineder, M. (n.d.). DEVELOPMENT OF A SCIENTIFIC PERMANENT SCATTERER SYSTEM: MODIFICATIONS FOR MIXED ERS/ENVISAT TIME SERIES. 9.

Bayramov, E., Tessari, G., & Kada, M. (2022). Quantifying Two-Dimensional Surface Displacements Using High-Resolution Cosmo-SkyMed, TerraSAR-X and Medium-Resolution Sentinel-1 SAR Interferometry: Case Study for the Tengiz Oilfield. Sensors, 22. https://doi.org/10.3390/s22176416

Dehghani, M., Valadan Zoej, M. J., Entezam, I., Mansourian, A., & Saatchi, S. (2009). InSAR monitoring of progressive land subsidence in Neyshabour, northeast Iran. Geophysical Journal International, 178(1), 47–56.

https://doi.org/10.1111/j.1365-246X.2009.04135.x

Dehghani, M., Valadan Zoej, M. J., Hooper, A., Hanssen, R. F., Entezam, I., & Saatchi, S. (2013). Hybrid conventional and Persistent Scatterer SAR interferometry for land subsidence monitoring in the Tehran Basin, Iran. ISPRS Journal of Photogrammetry and Remote Sensing, 79, 157–170. https://doi.org/10.1016/j.isprsjprs.2013.02.012

Ferretti, A., Prati, C., & Rocca, F. (2001). Permanent scatterers in SAR interferometry. IEEE Trans Geosci Remot Sen. Geoscience and Remote Sensing, IEEE Transactions On, 39, 8–20. https://doi.org/10.1109/36.898661

(Gini) Ketelaar, V. B. H. (2009). Satellite Radar Interferometry (Vol. 14). Springer Netherlands. https://doi.org/10.1007/978-1-4020-9428-6

Hanssen, R. F. (2001a). Radar interferometry: Data interpretation and error analysis. https://repository.tudelft.nl/islandora/object/uuid%3Aa83859d5-c034-427e-b6a9-114c4b008d19

Hanssen, R. F. (2001b). Radar Interferometry: Data Interpretation and Error Analysis (Vol. 2). Springer Netherlands. https://doi.org/10.1007/0-306-47633-9

Hoeser, T. (2022). StaMPS-Visualizer [R]. https://github.com/thho/StaMPS_Visualizer (Original work published 2018)

Hooper, A. (2008). A multi-temporal InSAR method incorporating both persistent scatterer and small baseline approaches. Geophysical Research Letters, 35(16). https://doi.org/10.1029/2008GL034654

Hooper, A., Bekaert, D., Spaans, K., & Arıkan, M. (2012). Recent advances in SAR interferometry time series analysis for measuring crustal deformation. Tectonophysics, 514–517, 1–13. https://doi.org/10.1016/j.tecto.2011.10.013

Hooper, A., Zebker, H., Segall, P., & Kampes, B. (2004). A new method for measuring deformation on Volcanoes and other natural terrains using InSAR Persistent Scatterers. Geophyiscal Research Letters, 31, 1–5. https://doi.org/10.1029/2004GL021737

Liu, P., Li, Q., Li, Z., Hoey, T., Liu, Y., & Wang, C. (2015). Land Subsidence over Oilfields in the Yellow River Delta. Remote Sensing, 7(2), 2. https://doi.org/10.3390/rs70201540

Mirzaii, Z., Hasanlou, M., Samiei Esfahany, S., Rojhani, M., & Ajourlou, P. (2019). Land Subsidence Monitoring in Azar Oil Field Based on Time Series Analysis. 18. https://doi.org/10.3390/ECRS-3-06190

Motagh, M., Djamour, Y., Walter, T. R., Wetzel, H.-U., Zschau, J., & Arabi, S. (2007). Land subsidence in Mashhad Valley, northeast Iran: Results from InSAR, levelling and GPS. Geophysical Journal International, 168(2), 518–526. https://doi.org/10.1111/j.1365-246X.2006.03246.x

Motagh, M., Shamshiri, R., Haghshenas Haghighi, M., Wetzel, H.-U., Akbari, B., Nahavandchi, H., Roessner, S., & Arabi, S. (2017). Quantifying groundwater exploitation induced subsidence in the Rafsanjan plain, southeastern Iran, using InSAR time-series and in situ measurements. Engineering Geology, 218, 134–151. https://doi.org/10.1016/j.enggeo.2017.01.011

Motagh, M., Walter, T. R., Sharifi, M. A., Fielding, E., Schenk, A., Anderssohn, J., & Zschau, J. (2008). Land subsidence in Iran caused by widespread water-reservoir overexploitation. Geophysical Research Letters, 35, L16403. https://doi.org/10.1029/2008GL033814

Mousavi, S. M., Shamsai, A., Naggar, M. H. E., & Khamehchian, M. (2001). A GPS-based monitoring program of land subsidence due to groundwater withdrawal in Iran. Canadian Journal of Civil Engineering, 28(3), 452–464. https://doi.org/10.1139/l01-013

Samiei Esfahany, S., & Ajourlou, P. (2018, November 22). Monitoring local subsidence from 2014 to 2018 in Tehran using T-InSAR Sentinel1-A radar images (in Persian).

Shi, J., xu, B., Chen, Q., Miaowen, H., & Zeng, Y. (2022). Monitoring and analysing long-term vertical time-series deformation due to oil and gas extraction using multi-track SAR dataset: A study on lost hills oilfield. International Journal of Applied Earth Observation and Geoinformation, 107, 102679. https://doi.org/10.1016/j.jag.2022.102679

Siles, G. (2015). Advanced InSAR methodologies to study subsidence and fracturing caused by groundwater withdrawal in Valley of Mexico. https://doi.org/10.24355/dbbs.084-201504131130-0

SNAP Download – STEP. (n.d.). Retrieved December 13, 2022, from https://step.esa.int/main/download/snap download/

Sousa, J. J., Hooper, A. J., Hanssen, R. F., Bastos, L. C., & Ruiz, A. M. (2011). Persistent Scatterer InSAR: A comparison of methodologies based on a model of temporal deformation vs. spatial correlation selection criteria. Remote Sensing of Environment, 115(10), 2652–2663.

StaMPS. (n.d.). Retrieved December 13, 2022, from https://homepages.see.leeds.ac.uk/~earahoo/stam/

Fathollhi, N., & Hanzazi, M., & Bahroudi, A. (1397). Barrasi frouneshast zamin dar asare estekhraje mavade nafti ba estefade az raveshe tadakholsanji radar. Scientific – Research Quarterly Geographical Data (SEPEHR), 27th, No:105(in Persian).

https://civilica.com/doc/795768/

FouladiMogadam, N., & Metkan, A., & Sahebi, M., & Rostai, M. (2011). Ashkarsazi tagheershekle sathi bar payeye tadakholsanji tafazoli radar dar meydan nafti aghajari. Geological Survey of Iran. 20th, No.80 (in Persian).

https://doi.org/10.22071/gsj.2011.55238

Sharifikiya, M. (1391). Taeen mizan va damane frouneshast zamin be komak ravesh tadakholsanji radari(D-InSAR) dar dashte noug bahrman. Journal of Spatial Planning. No.77(in Persian).

https://magiran.com/p1097499

Mohammadi, A., & Ziyai, M., & Sohrabi, S., & FouladiMogadam, N. (1389). Arzyabi frouneshast va tarakom meydan nafti droud. 5th Conference of Applied Geology and the Environment.

https://civilica.com/doc/102238/